LAWRENCE
LIVERMORE
NATIONAL
LABORATORY

LLNL-JRNL-538314

EMITTANCE OF POSITRON BEAMS PRODUCED IN INTENSE LASER PLASMA INTERACTION

H. Chen, J. Sheppard, D. D. Meyerhofer, A. Hazi, S. Anderson, H. Baldis, R. Fedosejev, J. Gronberg, N. Izumi, S. Kerr, E. Marley, J. Park, R. Tommasini, S. Wilks, G. J. Williams

March 15, 2012

Physics of Plasmas

Disclaimer

This document was prepared as an account of work sponsored by an agency of the United States government. Neither the United States government nor Lawrence Livermore National Security, LLC, nor any of their employees makes any warranty, expressed or implied, or assumes any legal liability or responsibility for the accuracy, completeness, or usefulness of any information, apparatus, product, or process disclosed, or represents that its use would not infringe privately owned rights. Reference herein to any specific commercial product, process, or service by trade name, trademark, manufacturer, or otherwise does not necessarily constitute or imply its endorsement, recommendation, or favoring by the United States government or Lawrence Livermore National Security, LLC. The views and opinions of authors expressed herein do not necessarily state or reflect those of the United States government or Lawrence Livermore National Security, LLC, and shall not be used for advertising or product endorsement purposes.

EMITTANCE OF POSITRON BEAMS PRODUCED IN INTENSE LASER PLASMA INTERACTION

Hui Chen1, J. C. Sheppard2, D. D. Meyerhofer3, A. Hazi1, S. Anderson1, H. Baldis4, R. Fedosejev5, J. Gronberg1, N. Izumi1, S. Kerr5, E. Marley4, J. Park4, R. Tommasini1, S. Wilks1, G. J. Williams4

1. *Lawrence Livermore National Laboratory, Livermore, CA 94551*
2. *SLAC, Standford University, Menlo Park, CA 94025*
3. *Laboratory for Laser Energetics, University of Rochester, Rochester, NY 14623*
4. *University of California, Davis, CA 95616*
5. *University of Alberta, Alberta T6G 2R3, Canada*

In this Letter, we report the first measurement of the emittance of intense laser-produced positron beams. The emittance values were derived through measurements of positron beam divergence and source size for different peak positron energies from various laser conditions, and for one of these laser conditions we also used a one dimensional *pepper-pot* technique to refine the emittance value. The laser-produced positrons have a geometric emittance between 100 - 500 mm.mrad, comparable to the positron sources used at existing accelerators. With 10^{10}-10^{12} positrons per bunch, this low emittance beam, which is quasi-monoenergetic in the energy range of 5 – 20 MeV, may be useful as an alternative positron source for future accelerators.

PAC: 41.75.Fr, 41.75.Jv, 52.38.Kd, 29.27.Fh

Recent experiments have demonstrated that irradiating high-Z targets with intense short pulse lasers (~ps pulse duration, 10^{18}-10^{20} Wcm^{-2}) creates a large number (>10^{10}) of quasi-monoenergetic MeV positrons, with ~20-40 degree divergence angle at full-width at half maximum (FWHM) [1, 2]. This raised the possibility of using laser-generated positrons as an alternative source in linear accelerators. The interest in using laser-produced positrons as a new source rests on the potential advantages of a much reduced physical size, therefore smaller cost, as well as improved beam characteristics, such as particles per pulse, energy span and beam emittance [3-6]. These advantages are shared by another "table-top" electron accelerator concept based on laser wake-field acceleration [7, 8].

Conventional positron sources typically consist of a multi-GeV electron beam hitting a thick, high Z target. For example, the Stanford Linear Collider (SLC) [9-11] used a 120 Hz, 30 GeV, 30 kW electron beam in conjunction with a 24 mm thick, water cooled, W(90%)-Rh(10%) target to produce positrons. A 2–kilometer long linear accelerator was required to generate the electron drive beam. Up to $5x10^{10}$ positrons per bunch, in the energy range of 2-20 MeV and with geometric emittance of about 500 mm.mrad, were captured in the downstream accelerator system. (For consistency, throughout this paper, emittance (ε) refers to geometric emittance rather than the invariant emittance ($\varepsilon\gamma$)). The collected positron bunches were then accelerated to 1.2 GeV and transported to an emittance damping ring prior to injection into the accelerator proper.

In comparison, the electrons used to produce positrons with intense lasers are made simultaneously in similar high-Z targets at a rate of one shot per 30 minutes.

Irradiating a much smaller target (1 mm thick, 2 mm diameter) with a very short duration (few ps), intense laser pulse generates about 10^{11} positrons with energies between 5-20 MeV [1, 2]. The physics processes involved are the following. When an intense laser pulse illuminates a solid target, the laser electric and magnetic fields interact with the free electrons in the coronal plasma that is generated by the low-intensity laser prepulse (preceding the main pulse) at the front surface of the target. The majority of the absorbed laser energy goes into accelerating a fraction of the plasma electrons to energies greater than MeV — these hot electrons are the power source of pair generation. The pair process that is important in laser-produced plasmas is the Bethe-Heitler (BH) process [12], which dominates for thick high-Z targets [1, 13, 14]. The same physical process is dominant in accelerator-based positron sources. In the BH process, the laser-produced hot electrons make ~MeV-energy bremsstrahlung photons that create electron-positron pairs upon interacting with the nuclei. (In contrast, the direct process of pair-creation by an ultraintense laser produces pairs by the vacuum polarization caused by the strong electric field of the laser [15].) Given the comparable numbers of particles per pulse and the particle energies, a remaining question to be addressed is the emittance of laser-produced positron beams, and how it compares to the ~500 mm.mrad available at the SLC.

Geometric emittance, ε, is expressed as $\varepsilon^2=[<x^2><x'^2>-(<xx'>)^2]$, where x and x' are the particle's position and divergence along the x-axis, and the angle-brackets indicate averages over all the particles in the beam. An upper limit of emittance is given by $\varepsilon^2=\sigma_x\sigma_{x'}$, where σ_x and $\sigma_{x'}$ are the root-mean-square (rms) values of the source size and divergence angle, respectively. In this paper, we report the upper limit emittance for four

positron energies: 6, 12, 17, and 28 MeV. We also present the emittance value derived using the 1-D pepper pot method [16,17] at 12 MeV.

Given the combination of the very small laser focal spot (~10^{-2} mm) and the measured divergence of the positron beam in the range of 350-700 mrad (20-40 degrees), one might expect the positron emittance to be less than 10 mm.mrad. However, the actual source size and emittance of the laser-produced positron beam turn out to be much larger, as illustrated in Fig. 1(a). The reason for this is two-fold. First, the hot electrons produced in the laser focal spot spread laterally as they propagate through the target Therefore, at any depth into the target, the positrons are created in an area larger the laser focal spot. Second, because the positrons are produced inside the target via the BH processes as discussed above, we have previously estimated [1] that a large fraction (~90%) of the positrons annihilate inside the target, and only a small portion has sufficient kinetic energies to emerge from the target and be useable as a source. It is the lateral distribution of the escaping positrons at the rear surface of the target that determines the source size. Both the source size and angular divergence are affected by the initial laser-plasma interaction and the charged particle transport through the target, and therefore they both depend on the laser and target conditions. This paper shows that in our experiments the source size was ~300 - 700 μm (FWHM) and the measured beam divergence was ~20-40 degrees over a range of laser energies. The upper limit emittance of the laser-produced positron beam is therefore in the range of 100 - 500 mm.mrad, which is comparable to that of the SLC positron source.

The experiments were performed using 10 picosecond laser pulses at 1.054 μm wavelength from the Titan laser at the Lawrence Livermore National Laboratory [18],

and the Omega EP laser at Laboratory for Laser Energtics, University of Rochester [19]. Laser energies of 200-320 J (Titan) and 250 - 850 J (Omega EP) were focused into ~8 μm (Titan) and ~25 μm (Omega EP) diameter spots producing peak laser intensities from 5×10^{18} to 6×10^{19} W/cm^2. All targets were solid gold disks of 1 mm thickness.

The experimental set up is shown in Fig. 1(b). The primary diagnostic was a magnetic spectrometer to be able to separate the positrons from electrons and protons. The spectrometer was absolutely calibrated allowing the total number of electrons, positrons and their energies to be determined [20]. To evaluate the upper limit of positron emittance, we used linear slit arrays that were attached to the collimator of the spectrometer and oriented parallel to its magnetic field. We used two different slit arrays, one with 15 slits each 200 μm wide separated by 200 μm, and the other with variable width slits ranging 50 to 1000 μm, separated by 850 μm. Parallel to the magnetic field lines, the slit arrays not only imaged the source, but also served as a 1-D pepper-pot that has been extensively studied as a technique to measure the beam emittance [5, 17, 21]. The acceptance angle of each slit greatly exceeded the possible source projection (by a factor between 60 – 200), thus ensured un-obscured source imaging. As shown in Fig. 1(b), the angle between the beam axis and the axis of the spectrometer was varied to scan through the divergence half-angle of the whole beam. This procedure was needed because, at 105 - 300 mm away from the source, where the spectrometer was placed, the beam size was larger than the length of the slit arrays. The (s-polarized) laser with an axially symmetric intensity distribution was incident on the planar target along a direction close to the target normal, which resulted in symmetric electron generations, and

consequently an axially symmetric positron beam. As result, only half of the beam needed to be scanned in the experiment.

The angular divergence of the beam was measured by keeping the laser and target conditions constant while recording the beam intensity across the beam. The fluctuations of the laser energies (up to 20%) between shots were factored in linearly when the normalized intensity was calculated. The data of beam intensity vs. angle was well fitted by using a Gaussion function. Figure 2 shows the results for laser energy of ~300 J and pulse-width of 10 ps (laser intensity ~$5x10^{19}$ W/cm^2). The divergence angle (FWHM) was found to be about 20 ± 6 degrees. For these laser parameters, the positrons distribution is quasi-monoenergetic with the peak at ~12 MeV. This results from acceleration of the positrons by the sheath electric field at the back of the target [2]. The uncertainty in the fit of the angular distribution comes mostly from the scatter of the beam intensities, which likely resulted from the shot-to-shot variation of laser prepulse condition. Although the prepulse energy is often proportional to the laser energy in the main pulse, the dependence of positrons generation on the prepulse conditions is so complicated that a simple linear folding was not sufficient to include its effect on the positron beam intensity.

In a similar fashion, the angular divergence was also measured at the Omega EP laser using higher laser energy, ~850 J, at 10 ps pulse duration with the 2 mm-diameter, 1 mm-thick gold target. The FWHM angular divergence was ~22 degrees (see Fig. 2 inset). The peak of the positron energy distribution shifted to ~18 MeV due to the higher laser energy.

In addition to the angular divergence, we measured the positron (and electron) source sizes from penumbral images [22-24] produced by 200, 250 and 1000 μm-width slits (Fig. 3). In the penumbral imaging system, the extent of the image on detector is a convolution of source size, slit function, system magnification and detector resolution. As shown in Fig. 3, the hard edges of the 1000 μm-width slit project a penumbral image of the source on to the imaging plane. Assuming that the intensity profile of the source is approximated by a Gauss function, separation of the 12% to 88% intensity points of the penumbral image (δ1 and δ2) corresponds to FWHM of the source. De-convolution of these data from the slit function, system magnification and detector resolution gave the source size, which was determined at the energy corresponding to the peak of the distribution. We also verified the axial symmetry of the positron beam by taking source-size data with the slit array oriented parallel and perpendicular to the direction in which the angular scan was performed. The results showed the same image size along the two perpendicular directions, confirming the expected the axial symmetry of the positron beam.

The error in the source-size data comes from several factors such as slit dimension measurement, system magnification calculation, fitting procedure, statistics and detector pixel size. The most significant of these are the magnification and detector spatial resolution. The use of a magnetic spectrometer in the setup, although being necessary in separating the electrons and positrons, limited the magnification of the system to l/L =1.2 – 1.6 (see Fig. 1(b)) due to the relatively short drift distance from the imaging slit to the detector. In addition, the detector was a Fuji image plate (BAS-IP-2040 SR), which has a spatial resolution of about 80-150 μm HWHM [28-30] when

scanned at a pixel size between 50 and 100 μm. The combination of small magnification and detector resolution limited the resolution of the source size measurement to about ±120 μm, while a quadrature addition of all individual errors gave the total error of about ± 150 μm.

Fig. 3 (inset) shows the positron source size as a function of energy (at the peak of its distribution) The source size varies between 800 and 400 um for peak energies between 6.5 MeV and 16 MeV MeV, with the larger source sizes corresponding to smaller peak energies. A possible explanation for this trend is that it results from collimation of the hot electrons by self-generated B field [25-27]. Higher peak positron energy means that higher flux of hot electrons is present, which produces a higher current, J, and a correspondingly larger B field. This field could reduce the angular spread of the electrons that generate the positrons via the HB process.

From the measured positron beam divergence and beam source size we derived the upper limit of the geometric emittance (at the peak of the positron energy distribution) for a number of laser energies as shown in Fig. 4. Also plotted in Fig. 4 is the result obtained from a detailed analysis of the emittance measurements made at laser energy of ~300 J, 10 ps. This analysis followed the well-defined 1-D pepper-pot equations derived in [17].

$$\varepsilon_x^2 = \frac{1}{N}\left\{\left[\sum_j^s n_j\left(x_j - \bar{x}\right)^2\right]\left[\sum_j^s n_j\left[\sigma_{j,x'}^2 + \left(x'_j - \bar{x}'\right)^2\right]\right] - \left[\sum_j^s n_j x_j x'_j - N\,\bar{x}\,\bar{x}'\right]^2\right\}$$

where N is the total number of positrons through the slits $N = \sum_j^s n_j$ and n_j is the number of positrons through the j^{th} slit. x_j and x'_j are the position and divergence of the

slit j, whereas $\bar{x}$ and $\bar{x}'$ denote the mean slit position, the mean divergence, respectively. $\sigma_{j,x'}^2$ is the root-mean-square divergence of the beamlet j. We added the correction to $\sigma_{j,x'}^2$ resulting from the flattop distribution created by the slit projection [5, 21]:

$$\sigma_{j,x'}^2 = \frac{\sigma_j^2 - \left(Md/\sqrt{12}\right)^2}{L^2}, \text{ and } M = (L+l)/l$$

where l is the distance from the source to the slits, and L from the slits to the image plane. M is then the magnification of the system, and d is the width of the slit. Using the measured data points in above equation, we obtained 100.5 ± 44 mm.mrad for the emittance of the whole beam. If one were to interpolate the beam intensity at various angles through a Gaussian fit of the data points, a slightly smaller total beam emittance of 62.3 ±58 mm.mrad would result for such an idealized case.

Overall, the emittance of laser-produced positrons is comparable to but somewhat smaller than that of the 480 mm.mrad source used at SLC (Fig. 4). It is interesting to note that, although the physical process of positron generation is the same for the laser and the accelerator, processes unique to intense laser-plasma interactions may have helped to limit the beam emittance in at least two ways. First, the laser focal spot is very small (~10 μm) limiting the source size of the electrons that ultimately generate the positrons, and the "cone of birth" of the positrons may have been further decreased by a plasma pinch effect. Secondly, the sheath acceleration experienced by the positrons at the rear surface of the target not only provides a favorable monoenergetic distribution, but also acts like a longitudinal stretcher, which elongates the positron cone and effectively reduces the beam divergence. However, in comparison with the emittance of wakefield-accelerated

electron beams [3-5] or that of laser-produced proton beams [6], the positron emittance is much larger. Although both the positrons and protons are accelerated by the "target normal sheet acceleration" mechanism [31] at the rear surface of solid high-Z targets, when irradiated by short, intense laser pulses at 10^{18}-10^{20} Wcm^{-2}, their "birth" place and "birth" divergence are quite different. The protons are created by the same sheath field via ionization of hydrogen atoms on the surface (present as hydrogen-containing contaminants). Their source size, divergence, and hence emittance, is determined primarily by the strength of the sheath field as a function of space and time. [32]. On the other hand, the positrons are created inside the target via the HB process, and both their "birth" place, divergence and transport through the target to the surface (prior to acceleration by the sheath field) are important factors in determining their source size and emittance.

Despite the fact that the positron numbers, energies and emittance are favorable for laser-produced positrons as an alternative source for accelerators, the present state of high intensity-laser technologies seriously limits this application. Specifically, the low repetition rate of current laser-produced positron sources is such that it cannot yet meet the needs of an accelerator. In general, the positron sources for accelerators need to operate at 5 – 120 HZ [33]. There are, however, substantial efforts under way worldwide to develop high power lasers with 0.1 - 10 HZ repetition rates driven by various needs [34, 35]. Such advances in laser technology, when realized, should enable laser-generated positrons to be an alternative accelerator source in the foreseeable future.

In conclusion, the emittance of positron beams from intense laser-plasma interactions was measured to be in the range from 100 to 500 mm.mrad for energies

between 6 and 20 MeV. This is comparable to but somewhat smaller than the emittance of the positron source used at the SLC accelerator. Although with a much lower repetition rate, laser produced positron beams with their comparable emittance, large particle number and quasi-mono-energetic particle energies per pulse make it useful as an alternative source for future accelerate.

Acknowledgement: We would like to thank Dr. Tor Raubenheimer (SLAC) for initiating this work, and Drs. Peter Beiersdorfer, Bob Cauble, Henry Shaw and Bill Goldstein for their encouragement and support. We gratefully acknowledge the JLF and Omega EP facility support during the experiment. Part of this work was performed under the auspices of the U.S. DOE by LLNL under Contract DE-AC52-07NA27344, and funded by the LLNL LDRD program (10-ERD-044).

[1] Hui Chen, et al., Phys. Rev. Lett. **105**, 015003 (2010)

[2] Hui Chen, et al., Phys. Rev. Lett. **102**, 105001 (2009)

[3] E. Brunetti, et al., Phys. Rev. Lett. **105**, 215007 (2010)

[4] S. Fritzler, et al., Phys. Rev. Lett. **92**, 165006 (2004)

[5] C. M. S. Sears, et al., Phys. Rev. Special Topics–Accelerators and Beams, **13**, 092803 (2010)

[6] T. E. Cowan, et al., Phys. Rev. Lett. **92**, 204801 (2004)

[7] C. Joshi and E. Malka, New J. Phys. **12**, 045003 (2010)

[8] V. Malka, Phys. Plasmas, in print (2012)

[9] S. D. Ecklund, SLAC-PUB-4437

[10] V. Bharadwaj, et al., Proceedings of 2005 Particle Accelerator Conference, Knoxville, Tennessee, p3230 (2005)

[11] J. C. Sheppard, et al., IEEE Transactions on Nuclear Science, Vol. **NS-30**, 2161 (1983)

[12] W. Heitler, The Quantum Theory of Radiation (Clarendon Press, Oxford, 1954)

[13] K. Nakashima and H.Takabe, Phys. Plasmas **9**, 1505 (2002)

[14] Y. H. Yan, et al., Phys. Plasmas **19**, 023114 (2012)

[15] D. L. Burke, et al., Phys. Rev. Lett. **79**, 1626 (1997)

[16] Y. Yamazaki, et al., Nuclear Instrum. And Methods in Phys. Research, **A322**, 139 (1992)

[17] M. Zhang, "Emittance formula for slits and pepper-pot measurements", Fermi National Accelerator Laboratory, Fermilab-TM-1988, (1996)

[18] B. C. Stuart et al., in Conference on Lasers and Electro-Optics/Quantum Electronics and Laser Science Con- ference and Photonic Applications Systems Technologies,

Technical Digest (CD) (Optical Society of America, Long Beach, CA, 2006), paper JTuG3.

[19] L. J. Waxer et al., Opt. Photonics News **16**, 30 (2005).

[20] Hui Chen, et al., Rev. Sci. Instrum. **79**, 033301 (2008)

[21] S. G. Anderson et al., Phys. Rev. Special Topics – Accelerators and Beams, **5**, 014201 (2002)

[22] K. A. Nugent and B. Luther-Davies, Optics Communications, **49,** 393 (1984), and Applied Optics, **25**, 1008 (1986).

[23] R. Azuma, et al., Rev. Sci. Instrum. **81**, 10E517 (2010)

[24] S. Nozaki, et al., Rev. Sci. Instrum. **73**, 3198 (2002)

[25] A. R. Bell and R. J. Kingham, Phys. Rev. Lett. **91**, 035003 (2003)

[26] M. Storm, et al.,, Phys. Rev. Lett. **102**, 235004 (2009)

[27] Y. Sentoku, et al., Phys. Rev. Lett. **107**, 135005 (2011)

[28] B. R. Maddox, et al., Rev. Sci. Instrum. 82, 023111 (2011)

[29] S. G. Gales and C. D. Bentley, Rev. Sci. Instrum. **75**, 4001 (2004)

[30] N. Izumi, et al., Rev. Sci. Instrum. **77**, 10E325 (2006)

[31] S. C. Wilks, et al., Phys. Plasmas **8**, 542 (2001)

[32] A. J. Kemp, et al, Phys. Rev. E **75**, 056401 (2007)

[33] T. Raubenheimer, et al., private communication, SLAC (2009)

[34] Mike Dunne et all, "HiPER Technical Background and Conceptual Design Report 2007", June 2007; http://www.hiperlaser.org/

[35] J. Faure, et al., Phys. Plasmas **17**, 083107 (2010)

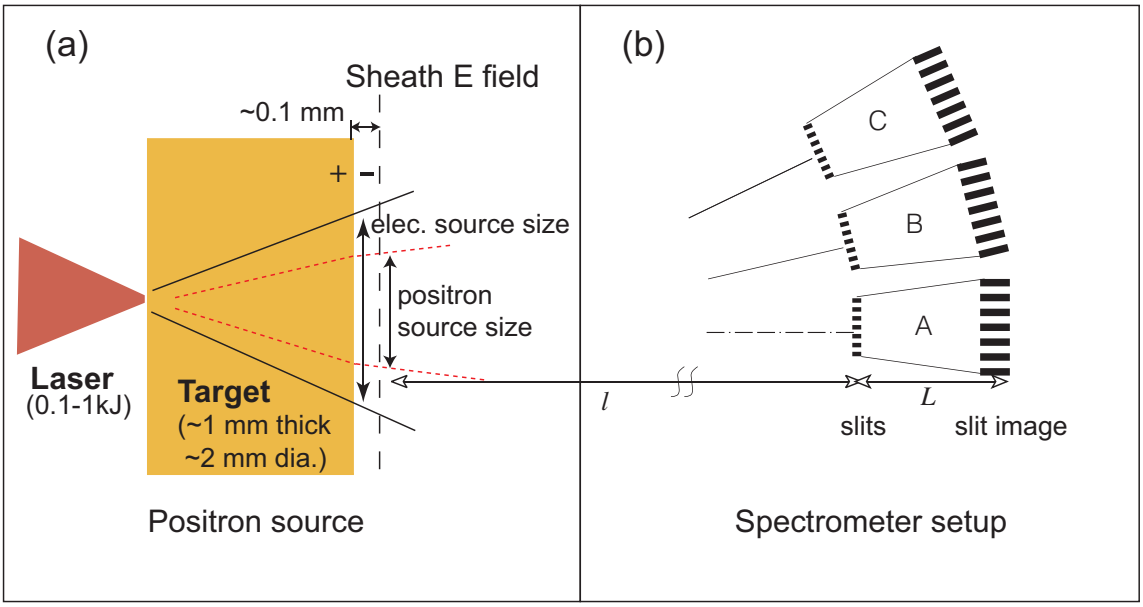

FIG. 1: Schematic of laser and target geometry (a) and positron emittance measurement setup (b) (not to scale). Positron (and electron) source refers to those particles that emerge from the rear surface of the target. The emittance measurements were made at various positions (denoted A, B and C) to cover half of the angular divergence of the whole beam, while for a given position each slit covers only a small portion of the beam.

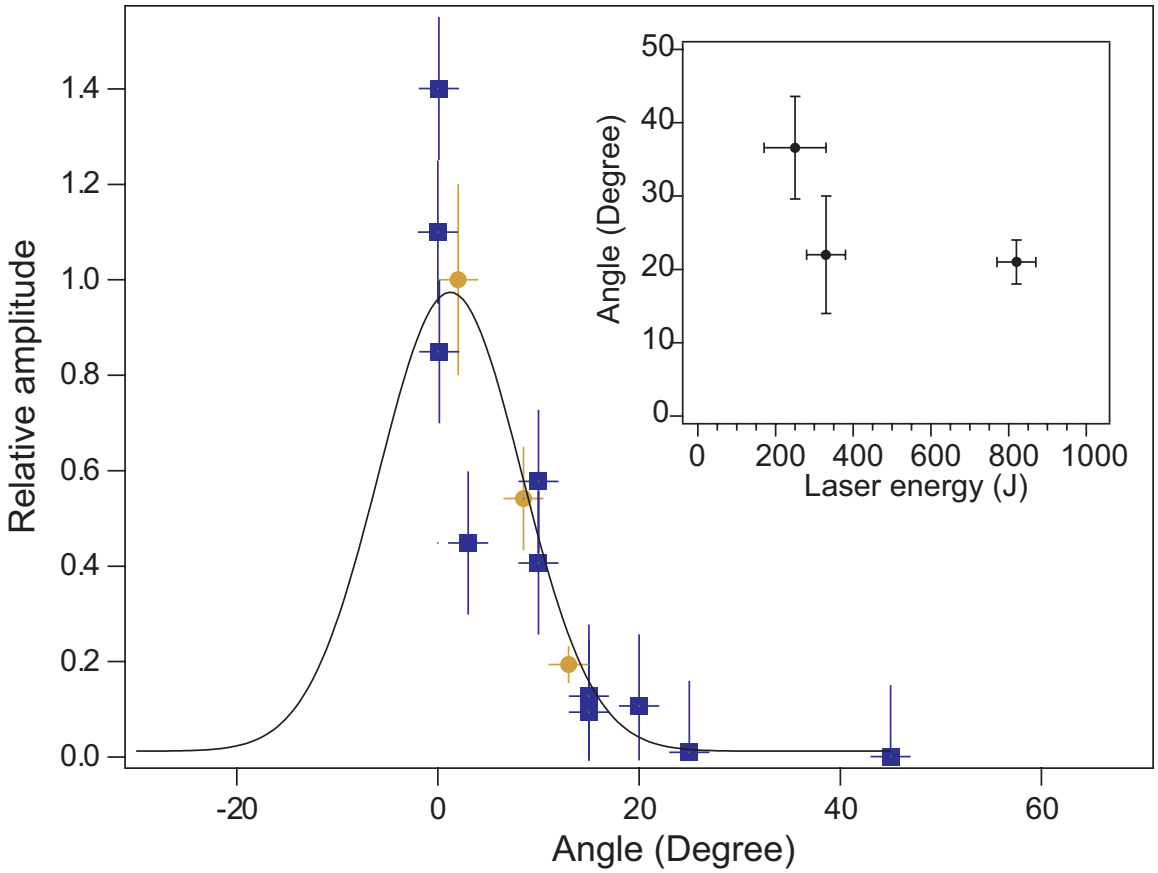

FIG. 2: Angular divergence of the positron beam measured at Titan laser with laser energy of ~300 J, and pulse duration of 10 ps. The positron energy at the peak of distribution was 12 MeV. The inset figure is the angular divergence of positron beam as a function of laser energy. The data for laser energies less than 400 J were obtained at Titan, and for ~800 J at Omega EP.

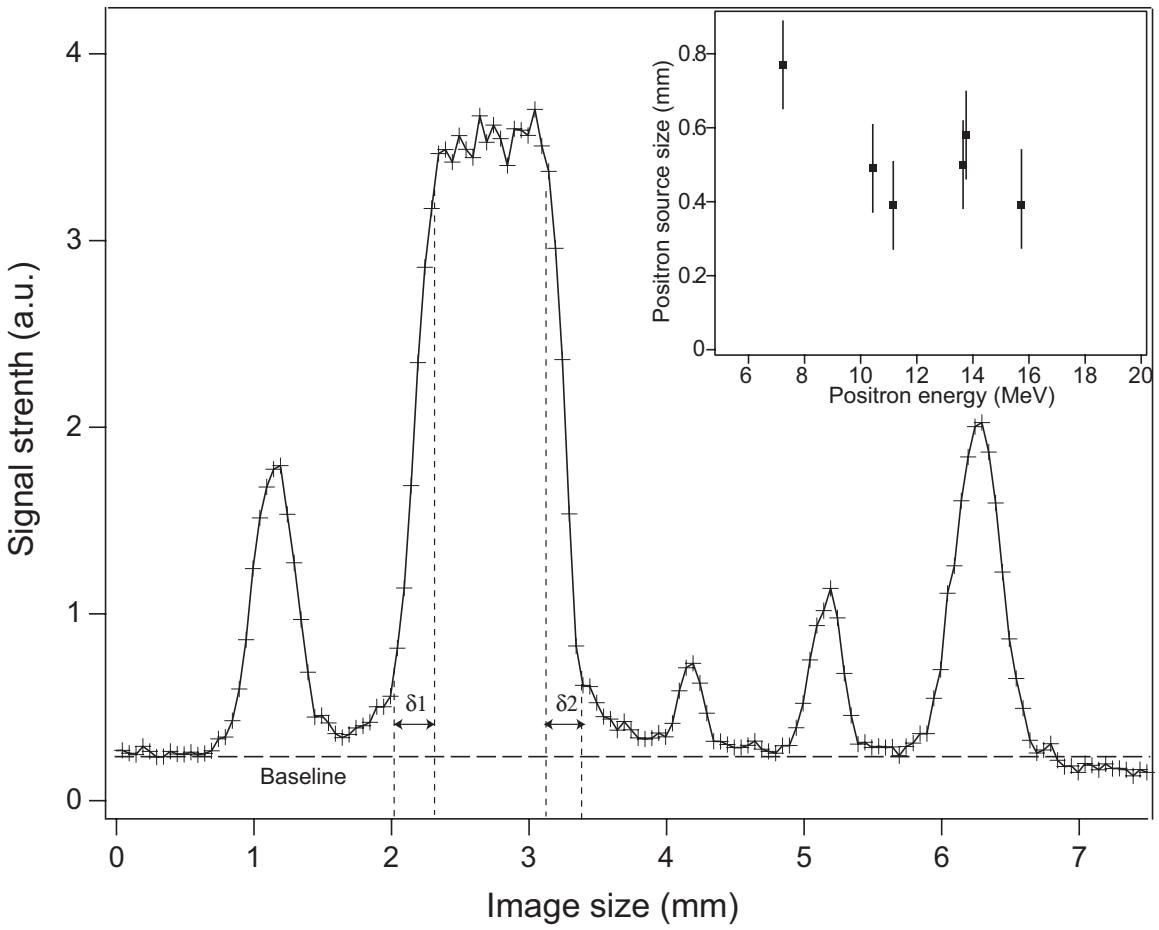

FIG. 3: Lineout of the image of the positron beam through a slit array with variable slit-width of 200, 1000, 50, 100, 250 μm, from left to right. The average of δ1 and δ2, taken between 12%-88% height of the maximum amplitude was used to infer the source size. The inset shows the measured positron source size as a function of positron energy (taken at the peak of the positron energy distribution) for several laser shots. at Titan under various laser conditions.

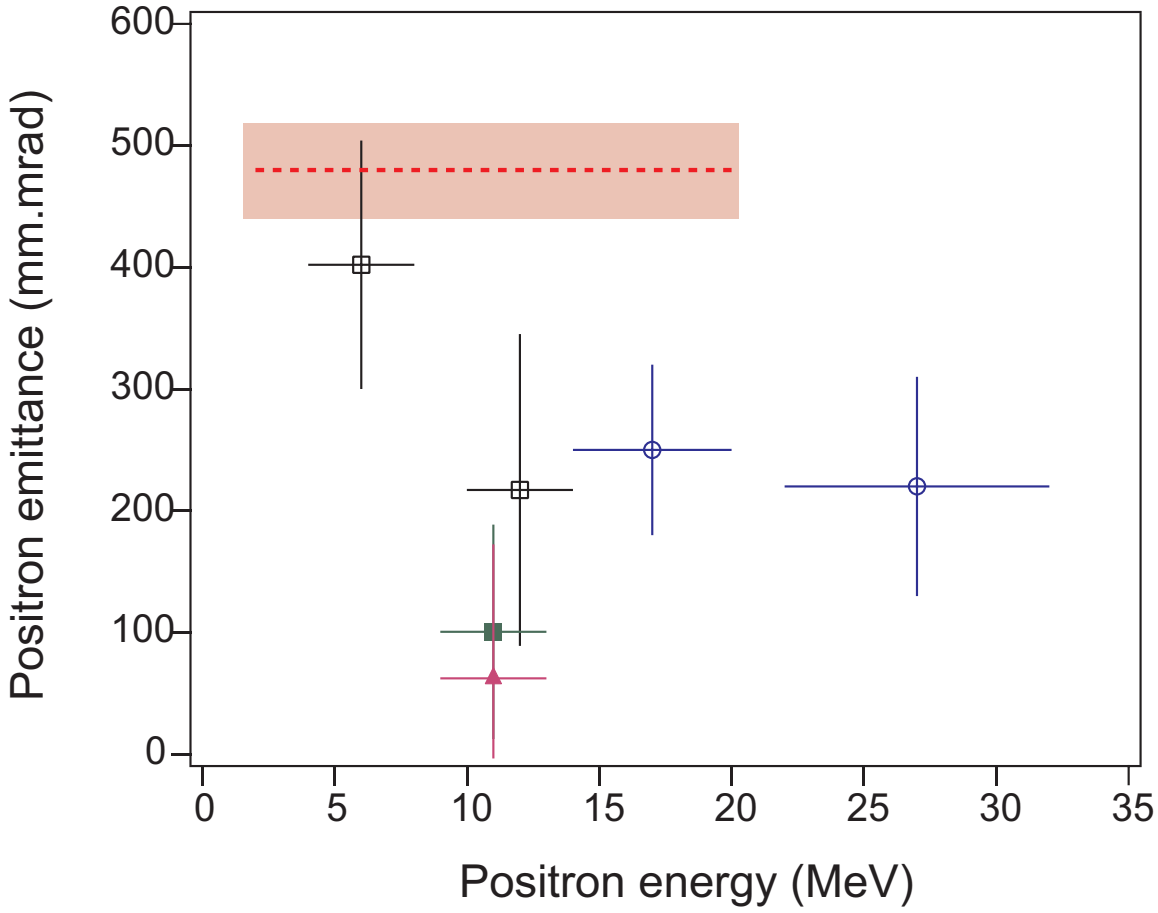

Fig. 4. Summary of the measured emittance of laser-produced positrons in comparison to that of SLC. The open squares and open circles denote the upper limit emittance determined from beam divergence and source size measurements on Titan and Omega EP lasers, respectively. The solid square and solid triangle were derived from 1-D pepper-pot analysis of the Titan data at ~12 MeV using the measured data points and using a continuous fit of these data points, respectively. The latter two data points were arbitrarily shifted to 11 MeV to make the figure more legible. The SLC positron emittance and its expansion range are plotted as dashed line and surrounding shadow.